

EFFECT OF BIOSYNTHESIZED SILVER NANOPARTICLES ON THE OPTICAL, STRUCTURAL, AND MORPHOLOGICAL PROPERTIES OF TiO₂ NANOCRYSTALS

Jamila Tasiu^a, Muhammad Y. Onimisi^b,  Abubakar S. Yusuf^c,  Eli Danladi^{d*}, Nicholas N. Tasiu^e

^a Department of Physics, Kaduna State University, Kaduna, Nigeria

^b Department of Physics, Nigerian Defence Academy, Kaduna, Nigeria

^c Department of Physics, Federal University of Technology, P.M.B 65, Minna, Nigeria State, Nigeria

^d Department of Physics, Federal University of Health Sciences, Otuipo, Benue State, Nigeria

^e Department of Physics, Rivers State University, Port Harcourt, Rivers State, Nigeria

*Corresponding Author e-mail: danladielibako@gmail.com

Received October 28, 2023; revised December 6, 2023; accepted December 8, 2023

The development of efficient metal doped semiconductors for Photovoltaic applications has gained a lot of research attention. In this present paper, pure and silver nanoparticles (AgNPs)-modified TiO₂ nanocrystals (NCs) with different amount of AgNPs (say 50, 100, 150, 200, and 250 μ L) were achieved and the effects of AgNPs on the TiO₂ NCs were explored systematically. The optical, structural and morphological properties were probed using UV-visible spectrophotometer, X-ray diffraction (XRD), and scanning electron microscope (SEM). The results of the optical studies showed a characteristic peak of TiO₂ and the redshifting of the peak position was observed by introducing AgNPs. The synergetic effects from AgNPs and TiO₂ results to diminished band gap. The XRD result confirmed the formation of a tetragonal anatase TiO₂ phase with a decrease in crystallite size with increasing AgNPs content. The SEM images show enhanced nucleation and film growth with presence of shining surface which can be seen to contribute to good photon management by enhancing light scattering. The unadulterated TiO₂ and AgNPs-modified TiO₂ have spherical morphology and uniform size distribution ranging from 20 to 30 nm. This study established the view that surface modification of TiO₂ with AgNPs is a viable approach towards achieving an efficient light photocatalyst.

Keywords: AgNPs; TiO₂; Nanocomposites; LSPR Effect; Photocatalyst

PACS: 61.05.C-, 78.20.-e, 68.37.-d, 81.07.-b, 88.40.H-, 87.64.Ee

1. INTRODUCTION

Titanium dioxide (TiO₂) is a highly studied semiconductor due to its optoelectronic nature and high chemical stability [1] and has been proven to be one of the materials that have found applications in sensors, antireflective coatings, electrochromic devices, solar energy conversion [2] etc. Nanocrystalline TiO₂ is classified as one of the successful nanomaterials applied for photocatalytic and photoelectrochemical [3]. One of the disadvantages of TiO₂ is its wide band gap (for anatase phase is $E_g = 3.2$ eV, for rutile is 3.0 eV) that have made the absorption coefficient limited for applications in the visible region of the electromagnetic spectrum. As a result, altering the band gap of TiO₂ to render it photosensitive in the visible-light region of electromagnetic spectrum with low electron-hole recombination is considered a viable alternative in photocatalysis [4].

One of the path-way to improving the photocatalytic properties is incorporation of noble metal nanoparticles, such as Pt, Ag, Pd, Au, and alloys which can display plasmonic effect in TiO₂ matrix. This will render it active in visible light harvesting and charge carrier separation simultaneously without sacrificing its crystal quality [5,6].

When noble metals come in contact with TiO₂, they behave as electron reservoir suppressing the recombination rate and significantly enhance carrier life time [4]. Among the noble metals, silver nanoparticles (Ag NPs) have displayed some extra ordinary properties that makes it attractive for application in different catalyst. Amongst these properties are; unique physical, chemical, electronic, and optical properties [4,7,8]. Introducing AgNPs in the TiO₂ environment also results to increase in photocatalytic efficiency by interfacial charge transfer that takes place through Ti-Ag-O phase and the presence of oxygen vacancies [4,9]. During sunlight visible interaction with the AgNPs, surface plasmon resonance effect is displayed which drive the electron from AgNPs to TiO₂ or the vice versa and in turn enhance light harvesting due to frequency matching [10,11].

Different methods of fabricating Ag doped TiO₂ have been demonstrated. For instance, some studies have utilized a chemical reduction method to introduce Ag⁺ into TiO₂ NPs [9,12]. Photo reduction method was used by Yang et al. [13] to introduce silver nitrate (AgNO₃) into TiO₂ NPs under UV light. In another study by Zhou et al. [14], they fabricated Ag/Ag-doped TiO₂ using modified sol-hydrothermal method in the presence of NaOH as additive. Daniel et al. [1] used successive ionic layer absorption and reaction to introduce AgNPs in TiO₂. Although in the reported works, chemical route was utilized to fabricate Ag doped TiO₂ NCs.

In our present work, we reported the biosynthesis of AgNPs and its effect on TiO₂ nanocrystal. The effect of the Ag nanoparticles on the optical, structural, and morphological was explored in a systematic way. The results showed that on introducing different amount of AgNPs through spin coating, the band optical properties of TiO₂ matrix were enhanced resulting to diminished bandgap of TiO₂ which presents good prospects for photocatalytic activity and photovoltaic

applications. This entire paper is presented in four sections. After the introduction section is the materials and method section, which offers a full description related to the synthesis and fabrication techniques. Section 3, includes the results and discussion. The conclusion section includes a summary of the findings.

2. MATERIALS AND METHODS

2.1. Materials

Ti-Nanoxide (T/SP36) was purchased from solaronix, Methanol (99.8%), Silver nitrate (99%), the commercial titanium dioxide (99.5%), Degussa P25, Sodium hydroxide (98.5%), were supplied by Sigma Aldrich. All the chemicals were of analytical grade and used as received without any further purification.

2.2. Preparation of Titanium dioxide

The Titanium Nanoxide T/SP 36 was diluted in absolute ethanol in the ratio 1:3 respectively to obtain the required composition. The prepared TiO₂ solution was sealed with aluminum foil to prevent it from absorbing moisture.

2.2. Preparation of biosynthesized AgNPs

The silver nanoparticle (AgNPs) was made in a green synthetic way using soluble starch as a reducing agent. In a typical one-step synthesis protocol, 0.5 g of soluble starch was added to 50 mL of deionized water and gently heated under continues stirring on hotplate at 100°C for 30 minutes. Later 0.01 M, 50 mL of AgNO₃ was added to the mixture and continued boiling at 90°C for 6 hours on hotplate with stirring. The colour of the silver nitrate solution changed from colourless to brownish yellow which indicate the formation of AgNPs. The obtained AgNPs were purified through repeated centrifugation at 11500 rpm for 20 minutes. AgNPs were collected and redispersed in deionized water.

2.3. Quantitation of the biosynthesized AgNPs

The concentration of AgNPs was estimated from concentration of AgNO₃ solution (0.01 M, 50 mL) following a procedure earlier described by Kalishwaralal et al. [15], and Rani et al. [16]

Step 1: Average number of atoms per nanoparticle (N):

From the synthesis we assumed that 100% of the silver atoms were converted into AgNPs

$$N = \frac{\pi \rho D^3}{6M} N_A$$

Where $\pi=3.142$, ρ is the density of the face-centered cubic crystalline structure of silver (i.e., 10.5g/cm³) [16], D is the average diameter of AgNPs (18 nm), M is the atomic mass of silver (107.86 g), and N_A is the number of the atoms per mole (Avogadro's number = 6.023 6.023 × 10²³). Therefore;

$$N = \frac{3.142 \times 10.5 \times (1.8 \times 10^{-6})^3 \times 6.023 \times 10^{23}}{6 \times 107.8}$$

$$N = 179166$$

Step 2: Molar concentration of AgNPs solution:

$$C = \frac{N_T}{NVN_A}$$

Where N_T = product of the molarity of AgNO₃ and atoms present in one mole, N = number of atoms per nanoparticle (as calculated in step 1), and V is the volume of solution. Therefore;

$$C = \frac{0.01 \times 6.023 \times 10^{23}}{179166 \times 0.05 \times 6.023 \times 10^{23}}$$

$$C = 1.12 \times 10^{-6} \text{ M.L}^{-1} = 1120 \text{ nM}$$

2.4. Deposition of TiO₂ Layer

The TiO₂ liquid paste was spin-coated on the substrate using modified centrifuge machine at 3000 rpm for 15 seconds. The deposited TiO₂ was dried at 150°C for 5 minutes and then annealed at 450°C for 30 minutes.

2.5 Silver nanoparticles deposition on TiO₂

Green synthesized metallic silver nanoparticles (AgNPs) was sputtered onto the surface of spin coated TiO₂ films by spin coating technique at room temperature. The silver content on the surface of the TiO₂ was varied by drop-casting 50, 100, 150, 200, and 250 μL. Immediately after the Ag deposition onto TiO₂, the films are annealed at 150°C for 5 minutes.

2.6 Films characterization

2.6.1 UV-vis spectrophotometer

UV-vis spectroscopy was performed to predict the charge transfer possibility between the acceptor and donor using Axiom Medicals (UV752 UV-Vis-NIR spectrophotometer) by scanning the absorption maxima of the mixture at wavelengths between 200–1200 nm.

2.6.2 X-ray diffraction (XRD)

The crystal structure of the nanoparticle films was performed on X-ray diffraction (Rigaku D, Max 2500) recorded in the 2 theta range from 10° to 70° and equipped with $CuK\alpha$ radiation ($\alpha = 1.54 \text{ \AA}$). The spectral data were operated at 40 kV and a current of 40 mA.

2.6.3. Scanning Electron Microscope (SEM)

Scanning Electron Microscope (SEM) was used to study the surface morphologies using JEOL (JSM-7600F) at a 20 kV acceleration voltage.

3. RESULTS AND DISCUSSION

3.1 Optical study

Figure 1a shows the curve of the absorbance against wavelength for pure TiO_2 and TiO_2 modified with different μL of AgNPs.

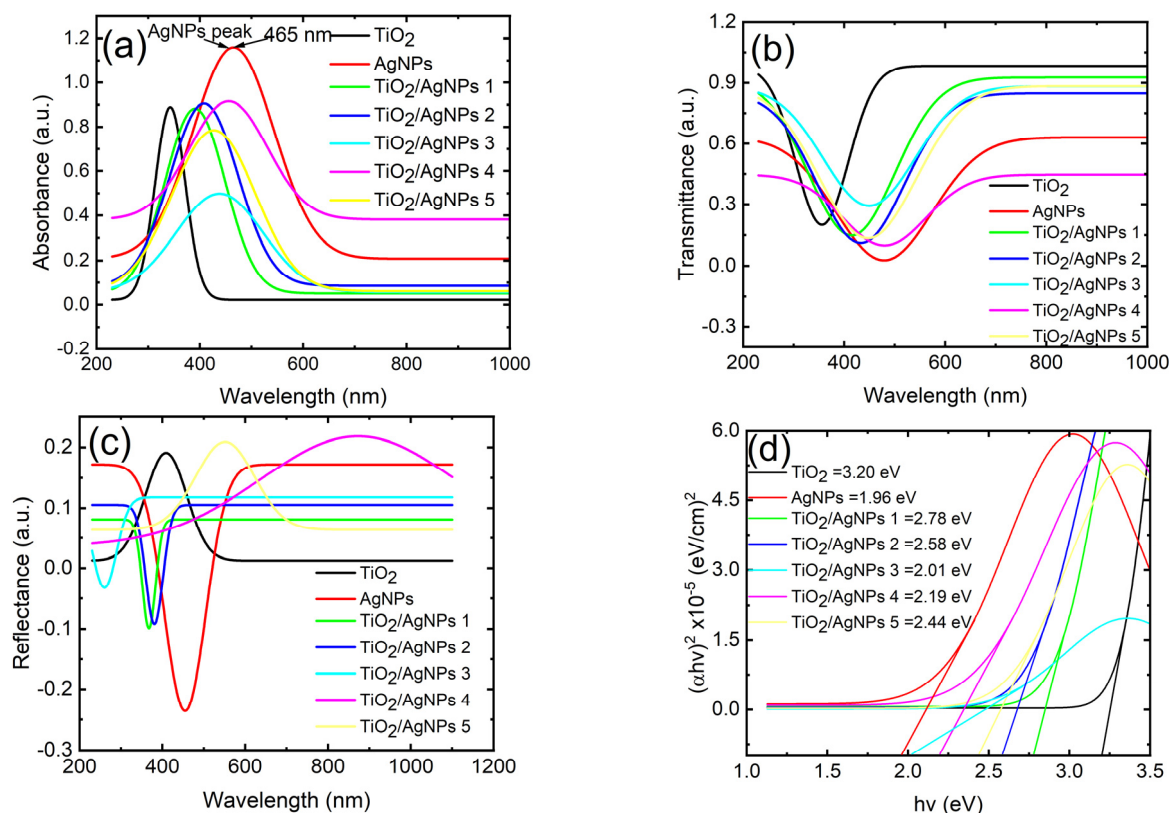


Figure 1. (a) Absorbance of TiO_2 , AgNPs, $TiO_2/AgNPs1$, $TiO_2/AgNPs2$, $TiO_2/AgNPs3$, $TiO_2/AgNPs4$, and $TiO_2/AgNPs5$, (b) Transmittance of TiO_2 , AgNPs, $TiO_2/AgNPs1$, $TiO_2/AgNPs2$, $TiO_2/AgNPs3$, $TiO_2/AgNPs4$, and $TiO_2/AgNPs5$, (c) Reflectance of TiO_2 , AgNPs, $TiO_2/AgNPs1$, $TiO_2/AgNPs2$, $TiO_2/AgNPs3$, $TiO_2/AgNPs4$, and $TiO_2/AgNPs5$, (d) Band gap energy of TiO_2 , AgNPs, $TiO_2/AgNPs1$, $TiO_2/AgNPs2$, $TiO_2/AgNPs3$, $TiO_2/AgNPs4$, and $TiO_2/AgNPs5$

Where AgNPs1=50 μL , AgNPs2=100 μL , AgNPs3=150 μL , AgNPs=200 μL , and AgNPs=250 μL

As it is seen from all the spectra, the curves modified with AgNPs show improved absorption in the visible range of the electromagnetic (em) spectrum. The titanium dioxide did not display any visible or near infrared peak, however an absorption peak between 278–405 nm in ultraviolet region with maximum peak at 341 nm was observed. This peak can be attributed to strong interaction between O 2p to Ti 3d charges [4]. As a result of the observed peak at the UV region, there is need to modify TiO_2 to make it active at the visible and near IR region.

On close inspection of the spectrum, the AgNPs shows a broad band with a visible peak observed at 465 nm which correspond to the plasmonic absorption of AgNPs [3,17–20]. The surface plasmon resonance effect is due to the mutual oscillation of conduction electrons which are in resonance with the light wave. The sample containing AgNPs is depicted to show a redshift in visible light matching which is attributed to surface plasmon resonance effect.

The TiO₂/AgNPs1 film shows a peak at 395 while the TiO₂/AgNPs2 film shows a further shift to 407 nm. On increasing the AgNPs drops to 3 and 4, we observed a redshift in the spectra with absorption peak of 440 nm and 460 nm. Further increase to 5 drops results to a blue shift in optical absorption which is attributed to photodegradation due to higher surface adsorption.

The optical transmittance of the samples is shown in Figure 1b which was obtained from equation 1.

$$T = 10^{-A} \tag{1}$$

where T is transmittance and A is absorbance.

As seen from the curve, at wavelengths between 400 to 1000 nm, all samples with AgNPs have lower transmittance than the sample without AgNPs. This differences in transmittance is attributed to the fact that the refractive index of TiO₂ is being more dispersive than those of AgNPs modified samples [21]. All the samples display high transparency in the visible region and near IR region with a sharp fall noticed at lower wavelength. The higher transmittance observed in pure TiO₂ than the AgNPs modified TiO₂ shows that, the introduction of AgNPs on TiO₂ increase the porosity of the film. We can attribute the possible reason of decrease in optical film density with increase in AgNPs content to this reason. The disparities in the transmittance of the film can be seen to arise mainly from the presence of different amount of AgNPs (50, 100, 150, 200, and 250 μL) introduced which results in inconsistencies in surface morphology, crystal size, and transmittance to light scattering [3,22].

The optical reflectance of pure TiO₂ and TiO₂ modified with different μL of AgNPs shown in Figure 1c were obtained from equation 2.

$$R = 1 - (A + T). \tag{2}$$

Where R is the reflectance, A is the absorbance and T is the transmittance

As depicted in the figure, all the films were seen to be reflective.

The reflectance was characterized with a peak and a valley. The presence of AgNPs with different content results to increase in porosity of the films which also causes a decrease in reflectance. This redshifting indicates that multiple light can scatter due to the pores as a result of introduction of AgNPs. This clearly means that, the unadulterated TiO₂ film shows a smaller porosity which enhances light reflectivity.

The optical band gap (E_g) was determined using the Tauc method which is a graph that expresses a relationship between $(\alpha h\nu)^2$ and $h\nu$. The extrapolation of the linear part $(\alpha h\nu)$ to zero point provides the band gap value.

The E_g were estimated utilizing the Tauc curve $(\alpha h\nu)^{1/r} = A[h\nu - E_g]$, where α = absorption coefficient, ν = incident photon frequency, E_g = bandgap, h = plank constant and A = constant, respectively. In the Tauc equation above, the value of r depends on optical absorption. For example, the transitions $1/2$ is known as direct allowed and 2 is known as indirect allowed, respectively, while the transitions 3 is known as direct forbidden and $3/2$ as indirect forbidden, respectively [23].

The band gap energy of the TiO₂ without AgNPs was 3.20 eV (see Figure 1d). Similar results have been reported by other researchers [1,3,24]. Upon incorporation of different μL of AgNPs, the band gaps were reduced to be 2.78, 2.58, 2.01, 2.19 and 2.44 eV for TiO₂, TiO₂/AgNPs1, TiO₂/AgNPs2, TiO₂/AgNPs3, TiO₂/AgNPs4 and TiO₂/AgNPs5 as depicted in Figure 1d. The AgNPs band gap is 1.95 eV. The reduced bandgap is as a result of increase in grain size due to increase in AgNPs content. This reduction has simply established the phenomenon of quantum size effects, in which the bigger the particle size, the smaller the bandgap [3,25].

3.2. Structural study

XRD patterns were studied to illustrate the structure and phase composition of the as synthesized nano materials. Figure 2a shows the XRD pattern of TiO₂ and TiO₂ modified with various μL of AgNPs and spin coated.

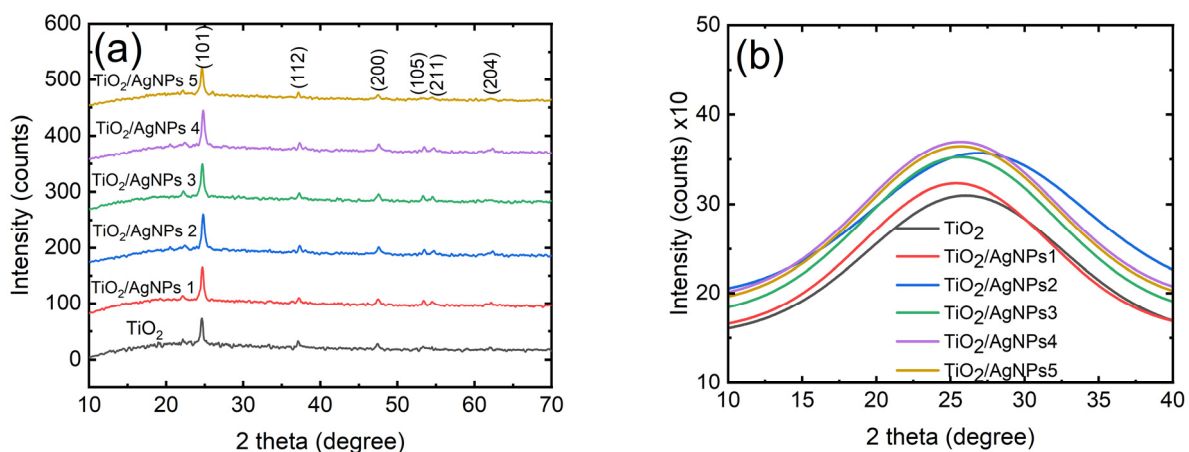


Figure 2. (a) – XRD pattern of TiO₂, and TiO₂ with different content of AgNPs; (b) – Gaussian fitted peaks for the most pronounced plane (101)

The creation of a tetragonal anatase TiO₂ phase was confirmed by all peaks in the pattern. The significant peaks at 24.59°, 37.22°, 47.88°, 53.42°, 54.53°, 62.21°, and 67.40°, which correspond to the planes (101), (112), (200), (105), (211), (204), and (116), respectively, are clearly visible. The peaks and planes exhibit great agreement with standard JCPDS card No. 89-4921 and also agrees with the findings reported by Danladi et al. [3] and Manju & Jawhar [26]. Anatase titania has been generated inevitably in all the films coated with the biosynthesized AgNPs, as evidenced by the absence of extra peaks due to AgNPs or comparable phases in the XRD plot. This only suggests that the addition of AgNPs improves the crystallinity of the film. AgNPs are introduced as a synthetic antenna, which alters the diffraction peak intensity and somewhat broadens the dominating peaks.

The peaks intensities increase with increasing drops of AgNPs except the film with 250 µL of AgNPs where the intensity is lower and this difference can be attributed to faster agglomeration rate of silver nanoparticles. We can see that, in relation to the AgNPs content increase, the high-intensity peak (101) position is somewhat pushed marginally into the higher angle position. To support our claim, the Gaussian fitted peaks for the most pronounced plane (101) are presented in Figure 2b.

The crystallite sizes (D) of all the pure and AgNPs modified films were estimated using equation 3 which is called the Debye–Scherrer equation [27]. All the parameters obtained are as shown in Table 1.

$$\text{Crystallite size } D = \frac{k\lambda}{\beta \cos\theta} \quad (3)$$

Table 1. Structural Parameters of TiO₂ and TiO₂ coated with 50, 100, 150, 200, and 250 µL of biosynthesized AgNPs.

| 2θ (degree) | hkl | Crystallite size (nm) | | | | | |
|-------------|-----|-----------------------|--------------------------|--------------------------|--------------------------|--------------------------|--------------------------|
| | | TiO ₂ | TiO ₂ /AgNPs1 | TiO ₂ /AgNPs2 | TiO ₂ /AgNPs3 | TiO ₂ /AgNPs4 | TiO ₂ /AgNPs5 |
| 23.46 | 101 | 3.87 | 5.02 | 4.69 | 4.28 | 4.27 | 4.54 |
| 37.36 | 112 | 11.94 | 9.92 | 10.74 | 10.95 | 10.46 | 9.57 |
| 47.13 | 200 | 10.41 | 11.39 | 6.51 | 8.19 | 7.47 | 8.68 |
| 53.36 | 105 | 42.82 | 38.63 | 24.97 | 28.11 | 17.45 | 32.97 |
| 54.38 | 211 | 8.22 | 30.38 | 41.28 | 12.24 | 22.89 | 17.37 |
| 61.08 | 204 | 19.51 | 2.43 | 10.99 | 45.18 | 11.32 | 35.45 |
| 67.92 | 116 | 5.49 | 12.39 | 5.49 | 5.34 | 9.71 | 3.11 |

3.3 Morphological Study

The morphological characteristics of the prepared films were studied using SEM micrographs.

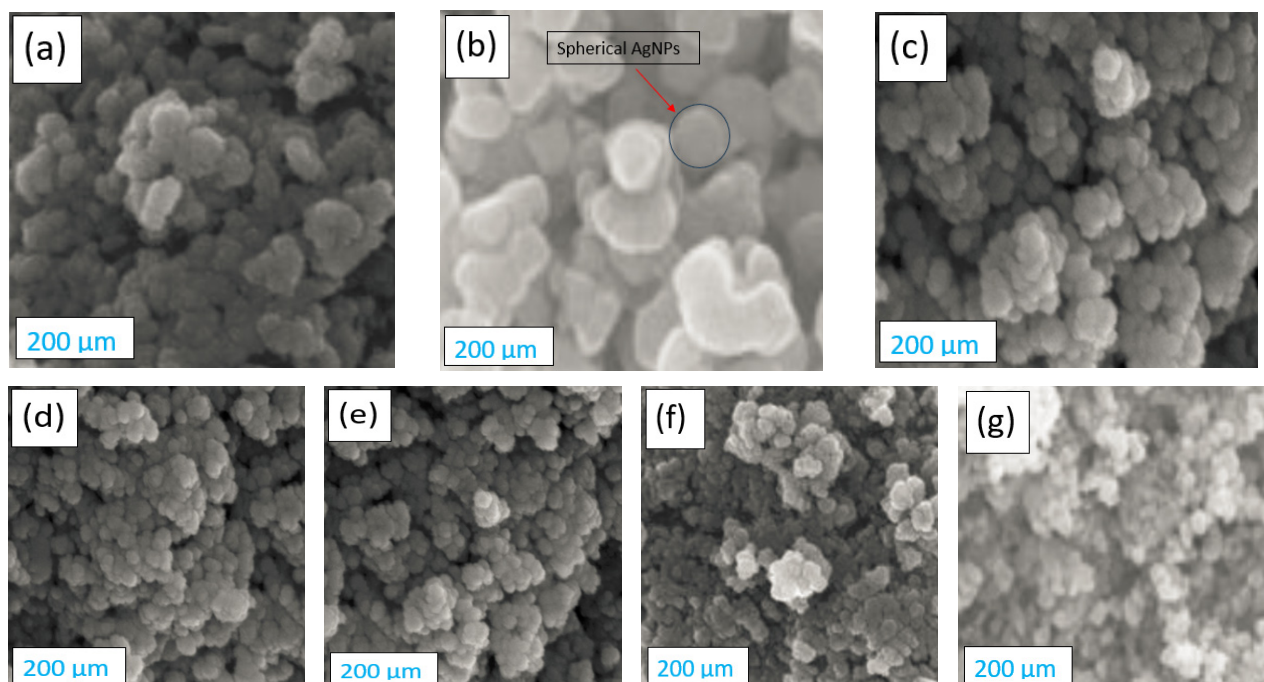


Figure 3. SEM images of (a) pure TiO₂, (b) Biosynthesized AgNPs, (c) TiO₂ with 50 µL of AgNPs, (d) TiO₂ with 100 µL of AgNPs, (e) TiO₂ with 150 µL of AgNPs, (f) TiO₂ with 200 µL of AgNPs and (g) TiO₂ with 250 µL of AgNPs

Figure 3a shows the SEM image of pure TiO₂, Figure 3b shows the SEM image of AgNPs, Figure 3c shows the SEM image of TiO₂/AgNPs1, Figure 3d shows the SEM image of TiO₂/AgNPs2, Figure 3e shows the SEM micrograph of TiO₂/AgNPs3, Figure 3f shows the SEM micrograph of TiO₂/AgNPs4 and Figure 3g shows the SEM micrograph of TiO₂/AgNPs5. The morphological structures of the films show well-densified surface which has spherical porosity. This

spherical porosity is an indication of the film to allow proper infiltration of the AgNPs into the space for good surface interaction. From the XRD data from Scherrer's formula and the SEM micrographs pattern, the sizes are in the nanoscale with the silver nanoparticles having average diameter of 18 nm.

Interestingly, the anchored Ag nanoparticles on the surface of TiO₂ is seen for the samples with Ag nanoparticles modification (Figure 3c-g) which further affirms the successful attachment of Ag nanoparticles on the surface of nanocrystalline TiO₂. As it is seen clearly, the micrographs with AgNPs show a shiny surface which display enhanced catalytic properties that can improve scattering of light and minimize recombination effect. The size of the AgNPs is controlled in our study by varying the μ L of AgNPs added in the TiO₂ nanocrystal. The size of the particle is increased with decreasing μ L of the AgNPs content added. This shows that the presence of AgNPs initiate nucleation with much film coverage. These different amount of AgNPs were utilized as light scattering layer in the modified films. From the structure, a greater aggregation was shown in the SEM image with 250 μ L of AgNPs which shows more islands formation and will subsequently results to less attachment at specific site of the titania. This by indication can lessen the catalytic effect and reduce the nucleation site that will give room for crystal film growth. We can relate this assertion with the XRD result of the film with 250 μ L of AgNPs where the intensity is lower due to faster agglomeration rate of silver nanoparticles.

4. CONCLUSION

In this study, pure TiO₂ and TiO₂ modified with AgNPs different μ L were successfully prepared and there optical, structural and morphological properties were probed using UV-visible spectrophotometer, X-ray diffraction (XRD), and scanning electron microscope (SEM). The optical properties detect surface plasmon resonance effect occurring at 465 nm which is the characteristic of surface plasmon resonance (SPR) of silver nanoparticles. The Ag incorporated TiO₂ films show a narrowed band gap and the Ag doping enhances the absorption of visible light due to plasmonic effect. XRD analysis reveals that the silver is crystallized in metallic state, and Ag nanoparticles are successfully formed in titanium dioxide matrix without indication of existence of Ag phases. As it is seen clearly, the micrographs with AgNPs show a shiny surface which display enhanced catalytic properties that can improve scattering of light and minimize recombination effect. This study established the view that deformation of TiO₂ with AgNPs is a good means towards achieving an efficient photocatalyst for photovoltaic application.

Conflict of interest. Authors have declared that there was no conflict of interest.

Funding. This article did not receive any funding support.

ORCID

©Eli Danladi, <https://orcid.org/0000-0001-5109-4690>; ©Abubakar S. Yusuf, <https://orcid.org/0000-0001-8181-9728>

REFERENCES

- [1] D. Thomas, E. Danladi, M.T. Ekwu, P.M. Gyuk, M.O. Abdulmalik, and I.O. Echi, *East European Journal of Physics*, **4**, 118 (2022). <https://doi.org/10.26565/2312-4334-2022-4-11>
- [2] T. Ivanova, A. Harizanova, T. Koutzarova, and B. Vertruyen, *Optical Materials*, **36**, 207 (2013). <https://doi.org/10.1016/j.optmat.2013.08.030>
- [3] E. Danladi, A. Ichoja, E. D. Onoja, D. S. Adepehin, E. E. Onwoke, O. M. Ekwu, and D. O. Alfred, *Materials Research Innovations*, **27**, 521 (2023). <https://doi.org/10.1080/14328917.2023.2204585>
- [4] F. Ahmed, M. B. Kanoun, C. Awada, C. Jonin, and P. F. Brevet, *Crystals*, **11**, 1488 (2021). <https://doi.org/10.3390/cryst11121488>
- [5] K. Wilke, and H. Breuer, *Journal of Photochemistry and Photobiology A*, **121**, 49 (1999). [https://doi.org/10.1016/S1010-6030\(98\)00452-3](https://doi.org/10.1016/S1010-6030(98)00452-3)
- [6] S. W. Verbruggen, M. Keulemans, M. Filippousi, D. Flahaut, G. V. Tendeloo, S. Lacombe, J. A. Martens, and S. Lenaerts, *Applied Catalysis B: Environmental*, **156–157**, 116 (2014). <https://doi.org/10.1016/j.apcatb.2014.03.027>
- [7] H. Zhang, C. Liang, J. Liu, Z. Tian, G. Wang, and W. Cai, *Langmuir*, **28**, 3938 (2012). <https://doi.org/10.1021/la2043526>
- [8] A. Subrahmanyam, K. Biju, P. Rajesh, K. J. Kumar, and M. R. Kiran, *Solar Energy Materials and Solar Cells*, **101**, 241 (2012). <https://doi.org/10.1016/j.solmat.2012.01.023>
- [9] D. Gogoi, A. Namdeo, A. K. Golder, and N. R. Peela, *International Journal of Hydrogen Energy*, **45**, 2729 (2020). <https://doi.org/10.1016/j.ijhydene.2019.11.127>
- [10] P. Wang, B. Huang, Y. Dai, and M.H. Whangbo, *Physical Chemistry Chemical Physics*, **14**, 9813 (2012). <https://doi.org/10.1039/C2CP40823F>
- [11] M. L. De Souza, D. P. dos Santos, and P. Corio, *RSC Advances*, **8**, 28753 (2018). <https://doi.org/10.1039/C8RA03919D>
- [12] Z. V. Quiñones-Jurado, M. Waldo-Mendoza, H. M. Aguilera-Bandin, E. G. Villabona-Leal, E. Cervantes-Gonzalez, and E. Pérez, *Materials Sciences and Applications*, **5**, 895 (2014). <http://dx.doi.org/10.4236/msa.2014.512091>
- [13] L. Yang, Q. Sang, J. Du, M. Yang, X. Li, Y. Shen, X. Han, X. Jiang, and B. Zhao, *Physical Chemistry Chemical Physics*, **20**, 15149 (2018). <https://doi.org/10.1039/C8CP01680A>
- [14] L. Zhou, J. Zhou, W. Lai, X. Yang, J. Meng, L. Su, C. Gu, T. Jiang, E. Y. B. Pun, and L. Shao, *Nature Communications*, **11**, 1785 (2020). <https://doi.org/10.1038/s41467-020-15484-6>
- [15] K. Kalishwaralal, S. BarathManiKanth, S.R.K. Pandian, V. Deepak, and S. Gurunathan, *Colloids Surfaces B Biointerfaces*, **79**, 340 (2010). <https://doi.org/10.1016/j.colsurfb.2010.04.014>
- [16] P. Rania, V. Kumar, P.P. Singh, A.S. Matharu, W. Zhang, K.H. Kimf, J. Singh, and M. Rawat, *Environment International*, **143**, 105924 (2020). <https://doi.org/10.1016/j.envint.2020.105924>
- [17] V. Katta, and R. Dubey, *Materialstoday: Proceedings*, **45**, 794 (2021). <https://doi.org/10.1016/j.matpr.2020.02.809>

- [18] M.G. González-Pedroza, A.R.T. Benítez, S.A. Navarro-Marchal, E. Martínez-Martínez, J.A. Marchal, H. Boulaiz, and R.A. Morales-Luckie, *Scientific Reports*, **13**, 790 (2023). <https://doi.org/10.1038/s41598-022-26818-3>
- [19] M. Madani, S. Hosny, D. M. Alshangiti, N. Nady, S. A. Alkhursani, H. Alkhalidi, S. A. Al-Gahtany, M. M. Ghobashy, and G. A. Gaber, *Nanotechnology Reviews*, **11**, 731 (2022). <https://doi.org/10.1515/ntrev-2022-0034>
- [20] Y. Khane, K. Benouis, S. Albukhaty, G. M. Sulaiman, M. M. Abomughaid, A. Al Ali, D. Aouf, F. Fenniche, S. Khane, W. Chaibi, A. Henni, H. D. Bouras, and N. Dizge, *Nanomaterials*, **12**, 2013 (2022). <https://doi.org/10.3390/nano12122013>
- [21] Y. M. Yeh, Y. S. Wang, and J. H. Li, *Optics Express*, **19**, A80 (2011). <https://doi.org/10.1364/OE.19.000A80>
- [22] P. Malliga, J. Pandiaraja, N. Prithivikumar, and K. Neyvasagam, *IOSR Journal of Applied Physics*, **6**, 22 (2014). <http://dx.doi.org/10.9790/4861-06112228>
- [23] F. Arjmand, Z. Golshani, S.J. Fatemi, S. Maghsoudi, A. Naeimi, and S.M.A. Hosseini, *Journal of Materials Research and Technology*, **18**, 1922 (2022). <https://doi.org/10.1016/j.jmrt.2022.03.088>
- [24] E. Danladi, M.Y. Onimisi, S. Garba, P.M. Gyuk, T. Jamila, and H.P. Boduku, *IOP Conference Series: Material Science and Engineering*, **805**, 012005 (2020). <https://doi.org/10.1088/1757-899X/805/1/012005>
- [25] M. Oztas, *Chinese Physics Letters*, **25**, 4090 (2008). <https://doi.org/10.1088/0256-307X/25/11/069>
- [26] J. Manju, and S. M. J. Jawhar, *Journal of Materials Research*, **33**, 1534 (2018). <https://doi.org/10.1557/jmr.2018.155>
- [27] A. Patterson, *Physical Review*, **56**, 978 (1939). <https://doi.org/10.1103/PhysRev.56.978>

ВПЛИВ БІОСИНТЕЗОВАНИХ НАНОЧАСТИНОК СРІБЛА НА ОПТИЧНІ, СТРУКТУРНІ ТА МОРФОЛОГІЧНІ ВЛАСТИВОСТІ НАНОКРИСТАЛІВ TiO₂

Джаміла Тасю^a, Мухаммад Й. Онімісі^b, Абубакар С. Юсуф^c, Елі Данладі^d, Ніколас Н. Тасі^e

^a Кафедра фізики, Університет штату Кадуна, Кадуна, Нігерія

^b Кафедра фізики Нігерійської оборонної академії, Кадуна, Нігерія

^c Факультет фізики, Федеральний технологічний університет, Р.М.В 65, Мінна, штат Нігерія, Нігерія

^d Факультет фізики, Федеральний університет наук про здоров'я, Отукно, штат Бенуе, Нігерія

^e Факультет фізики, Університет штату Ріверс, Порт-Гаркорт, штат Ріверс, Нігерія

Розробка ефективних легованих металом напівпровідників для фотоелектричних застосувань привернула велику увагу дослідників. У цьому документі було отримано чисті та модифіковані наночастинки срібла (AgNP) нанокристали TiO₂ (NC) з різною кількістю AgNP (скажімо; 1, 2, 3, 4 та 5 крапель), а також вплив AgNP на TiO₂ NCs. досліджено систематично. Оптичні, структурні та морфологічні властивості досліджували за допомогою УФ-видимого спектрофотометра, рентгенівської дифракції (XRD) та скануючого електронного мікроскопа (SEM). Результати оптичних досліджень показали характерний пік TiO₂, а червоне зміщення положення піку спостерігалось при введенні AgNPs. Синергетичний ефект від AgNP і TiO₂ призводить до зменшення забороненої зони. Результат XRD підтвердив утворення фази тетрагонального анатазу TiO₂ із зменшенням розміру кристалітів зі збільшенням вмісту AgNPs. Зображення SEM показують посилене зародження та ріст плівки з наявністю блискучої поверхні, яка, як видно, сприяє хорошему управлінню фотонами за рахунок посилення розсіювання світла. Чистий TiO₂ і модифікований AgNPs TiO₂ мають сферичну морфологію та рівномірний розподіл розмірів від 20 до 30 нм. Це дослідження встановило точку зору, що модифікація поверхні TiO₂ за допомогою AgNP є життєздатним підходом до досягнення ефективного світлового фотокаталізатора.

Ключові слова: AgNPs; TiO₂; нанокмозити; ефект LSPR; фотокаталізатор